Biosensors and Bioelectronics 53 (2014) 175–181

Contents lists available at ScienceDirect

Biosensors and Bioelectronics

journal homepage: www.elsevier.com/locate/bios

Photoelectrochemical biosensing platform for microRNA detection based on *in situ* producing electron donor from apoferritin-encapsulated ascorbic acid

Huanshun Yin [a], Mo Wang [a], Yunlei Zhou [a], Xiaoyan Zhang [a], Bing Sun [a], Guihua Wang [b,*], Shiyun Ai [a,**]

[a] College of Chemistry and Material Science, Shandong Agricultural University, 271018 Taian, Shandong, PR China
[b] College of Veterinary Medicine, Shandong Agricultural University, 271018 Taian, Shandong, PR China

ARTICLE INFO

Article history:
Received 2 August 2013
Received in revised form
24 September 2013
Accepted 24 September 2013
Available online 29 September 2013

Keywords:
Photoelectrochemical biosensor
MicroRNA detection
Bi_2S_3 nanorods
Avian leukosis viruses
Apoferritin

ABSTRACT

A novel signal "on" type of photoelectrochemical biosensor for microRNA-21 hybridization detection was fabricated, where Bi_2S_3 nanorods were used as photoactive material with a maximum adsorption at 450 nm visible light, hairpin-structure DNA as detecting probe, streptavidin as signal capturing unit and biotin functionalized ascorbic acid loaded apoferritin as signal amplification unit. Hybridization between the probe and the target microRNA-21 was confirmed by the increased photocurrent of the biosensor after electron donor of ascorbic acid was introduced into the detection buffer by digesting the apoferritin by trypsase, indicating that this method could be used f Prod. Type: FTPor quantitative measurements, and the discrimination of the complementary from mismatched microRNA-21. Under the optimal detection conditions, the photoelectrochemical biosensor displayed a linear range of 1–5000 fM and a low detection limit of 0.35 fM for microRNA-21 determination. Moreover, the down-regulated expression of microRNA-21 in poultry cells and tissues infecting with avian leukosis viruses was confirmed by directly detecting microRNA-21 in extracted total RNA. This proposed strategy may open a new avenue for the applications of photoelectrochemical biosensor for oligonucleotides detection using visible light irradiation, which could largely reduce the destructive effect of UV light on biomolecules.

1. Introduction

Avian leukosis (AL) is a kind of neoplastic disease, which is caused by avian leukosis viruses (ALVs). Up to now, AL has caused severe economic losses in breeding farms all over the world. Therefore, early detection and diagnosis of AL is very important for poultry farming and population purification. At present, the detection methods for AL are mainly located at ALVs detections (Hatai et al., 2009; Mohammadi et al., 2008; Zhang et al., 2010). However, the extraction and cetection process of ALVs might be hazardous to human, because the virus might mutate and infect people. Accordingly, development of a new biomarker for AL is necessary to reduce the risk.

MicroRNAs, a kind of small, endogenous, noncoding RNAs (~22 nucleotides), have been researched widely as biomarker for many cancers because microRNA was found to over-experssion or down-regulated expression in many cancers, such as stomach, prostate, esophagus, glioblastoma, neuroblastoma, cholangiocarcinoma, breast, lung, colorectal, and pancreatic cancer (Medina and Slack, 2008). Therefore, microRNA might be a perfect AL marker. To confirm it, the detection of expression level change of microRNA in poultry infecting with ALVs is necessary. So far, many techniques have been developed for microRNA detection, such as fluorescence (Yang et al., 2012), isothermal amplification (Zhang and Zhang, 2012), RT-PCR (Huang et al., 2009), microarrays (Yan et al., 2008), bioluminescence assay (Cissell et al., 2008), and electrochemistry (Pöhlmann and Sprinzl, 2010; Wu et al., 2013; Yang et al., 2009), etc. Though these methods have their own merits, the development of new detection technology for microRNA with high sensitivity and selectivity is still a challenge.

Photoelectrochemistry (PEC) is a newly developed analytical method, which has the advantages of both fluorescence and electrochemical sensors. In the PEC process, the light-induced current is used to quantify the target. Due to the separation of excitation source and detection signal, the sensitivity of the PEC is potentially high and some undesired background signals are reduced when comparing with conventional electrochemical and optical method (Dong et al., 2004). More importantly, PEC biosensor has manifested its promising application in DNA

* Corresponding author. Tel.: +86 538 8249248; fax: +86 538 8247660.
** Corresponding author.
E-mail addresses: wguihua1126@163.com (G. Wang), ashy@sdau.edu.cn (S. Ai).

0956-5663/$ - see front matter © 2013 Elsevier B.V. All rights reserved.
http://dx.doi.org/10.1016/j.bios.2013.09.053

analysis (Lu et al., 2008; Lu et al., 2006; Zhang et al., 2012a). Though PEC biosensors have been widely investigated and applied in biomolecules detection, only a few photoactive materials have been exploited and applied in PEC biosensors, such as TiO_2 (Li et al., 2011), CdS (Ding et al., 2010), CdTe (Wang et al., 2012b), CdSe (Zhang et al., 2011), WO_3 (Sun et al., 2013), BiOI (Gong et al., 2012), which might limit the development of PEC biosensor. Moreover, among these photoactive materials, only TiO_2 has been widely applied in PEC biosensor. However, the wide band gap of TiO_2 limits its direct applications in PEC biosensing since it can only absorbs UV light ($\lambda < 400$ nm) which can kill biomolecules (Kang et al., 2010). In order to overcome the shortcoming of TiO_2 as photoactive materials, TiO_2 was frequently modified with narrow-band gap semiconductors or organic photosensitizer, which could enhance the absorption in the visible range and increase the lifetime of charge carriers (Tu et al., 2010; Wang et al., 2009). But this modification will increase the experimental complexity. In addition, though semiconductor materials containing cadmium (such as CdS, CdTe and CdSe) have been successively applied in PEC biosensors, the Cd^{2+} is poisonous, which supplies the risk of environment pollution. For WO_3 and BiOI, the photocurrent rises from them needs to be further improved. Therefore, novel photoactive material should be developed and applied in PEC biosensors. And the novel photoactive material should have appropriate band energetic to absorb almost the entire visible region of the visible spectrum while maintaining its structural and electronic integrity.

Bismuth sulfide (Bi_2S_3) is known to be an attractive material for PEC application as it has a reasonably low band gap (Eg = 1.7 eV), an absorption coefficient in the order of 10^4 to 10^5 cm^{-1}, and a reasonable incident photon to electron conversion efficiency (~5%) (Peter et al., 2003; Tahir et al., 2010). It has been used as electrochemical hydrogen storage, hydrogen sensors, biomolecule detection, X-ray computed tomography imaging, and photoresponsive materials (Zhang et al., 2012b). More recently, it has been acted as a sensitizer due to its ability to absorb a large part of visible light up to 800 nm (Bessekhouad et al., 2004; Robert, 2007). Therefore, Bi_2S_3 should be a promising semiconductor material for PEC biosensors. Unfortunately, there is no report on its application in PEC biosensor for biomolecules detections.

In this work, we developed a novel signal "on" PEC biosensor for microRNA-21 detection, where Bi_2S_3 nanorods were used as photoactive material, hairpin-structure DNA as detecting probe, streptavidin as signal capturing unit and biotin functionalized ascorbic acid loaded apoferritin (Bio-AA-Apo) as signal amplification unit. It has been reported that apoferritin, a hollow spherical protein, is comprised of 24 subunits, with an interior and exterior diameter of 8 nm and 12 nm, respectively (Harrison and Arosio, 1996). It is interesting that the protein cage of apoferritin can be disassociated into 24 subunits when pH is lower than 2.0, and the subunits can recombine when pH is higher than 8.5. Apoferritin has been widely used as a protein cage to prepare size-restricted bio-inorganic or bio-organic nanocomposites. Some organic molecules, such as neutral red (Webb et al., 1994) and poly(ethylenimine) (Liao et al., 2012), have been captured in the cavities of apoferritin. Inspired by these researches, we synthesized ascorbic acid loaded apoferritin. As seen in Scheme 1, after the hairpin-structure DNA probe S1 was hybridized with microRNA-21, the retained single-strand fragment of probe DNA S1 (3′-end) further hybridized with biotin modified capture DNA S2. Subsequently,

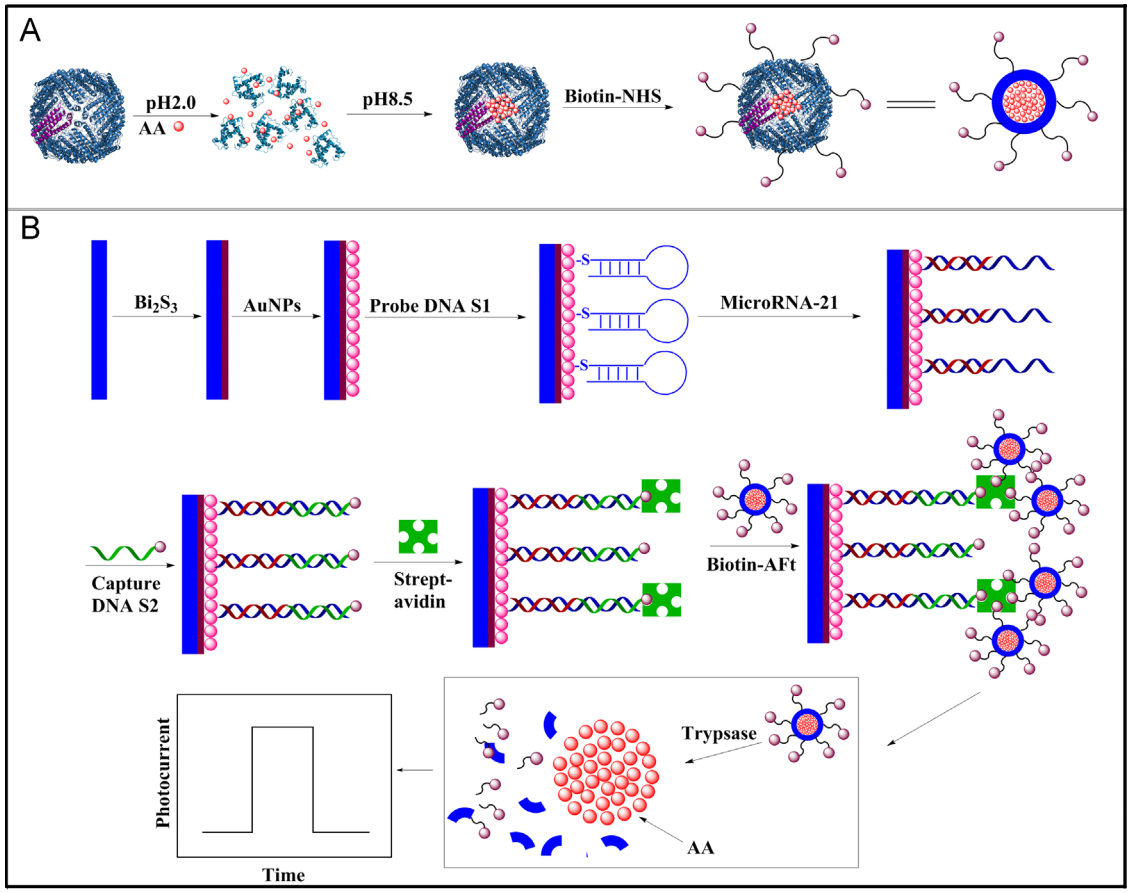

Scheme 1. Schematic representation of (A) the preparation of biotin functionalized ascorbic acid loaded apoferritin, and (B) photoelectrochemical biosensor fabrication and microRNA detection.

streptavidin was captured of the electrode surface based on bioaffinity reaction between biotin and strepavidin, which is a strong linkage in biological reactions. Finally, the assembly of Bio-AA-Apo on the electrode was achieved based on the reaction between biotin and strepavidin. When the electrode was immersed into detection buffer (0.1 M PBS, pH 7.8) containing trypsase, the immobilized aspoferritin could be catalytically hydrolyzed by trysase and the loaded AA could be released from the cavity of apoferritin into the detection buffer as sacrifice electron donor to arrest the photo-generated hole of Bi_2S_3, resulting in an increased photocurrent response. Because one strepavidin can integrate four biotins, more Bio-AA-Apo could be assembled on the electrode, the photocurrent response could be effectively amplified and the detection sensitivity was also improved.

2. Experimental section

2.1. Reagents and instruments

Apoferritin, biotin-NHS and streptavidin were purchased from Sigma (USA). Hydrogen tetrachloroaurate trihydrate ($HAuCl_4 \cdot 3H_2O$), tris(hydroxymethyl)aminomethane (Tris) and tris(2-carboxyethyl) phosphine hydrochloride (TCEP) were purchased from Aladdin (Shanghai, China). Mercaptopropionic acid (MPA) was obtained from Alfa Asear (USA). Diethypyrocarbonate (DEPC) and PEG-3350 were from Solarbio (China). AuNPs were synthesized according to previous report (Liu and Lu, 2006). The Apo-AA and Bio-AA-Apo were prepared according to previous reports with minor modifications (Liao et al., 2012; Liu et al., 2006a, 2006b) (see Supplementary materials). Bi_2S_3 nanorods were synthesized according to previous report with major modifications (Ge et al., 2012) (see Supplementary materials). Indium tin oxide (ITO) was purchased from Zhuhai Kaivo Electronic Components Co., Ltd. (Zhuhai, China, ITO coating 180 ± 25 nm, sheet resistance $< 15\ \Omega/cm^2$). Trypsase and all DNA sequences were purchased from Shanghai Sangon Biotechnology Co. (Shanghai, China) and used without further purification. MicroRNAs were synthesized and HPLC-purified by TaKaRa Biotechnology Co., Ltd. (Dalian, China). The oligonucleotides sequences were shown as follows. Probe DNA S1: 5′–SH $(CH_2)_6$-GGC CGT CAA CAT CAG TCT GAT AAG CTA AAC ATG ATA CGG CC-3′; MicroRNA-21: 5′–UAG CUU AUC AGA CUG AUG UUG A-3′; Capture DNA S2, 5′-biotin-GGC CGT ATC ATG TT-3′; single-base mismatched microRNA: 5′–UAG CUU A***A***C AGA CUG AUG UUG A-3′; three-base mismatched microRNA: 5′–UAG C***A***U AUC A***T***A CUG AUG ***C***UG A-3′; non-complementary microRNA: 5′–GUA AGG CAU CUG ACC GAA GGC A-3′. The nucleotide mismatches were indicated as italic and bold letters. Synthetic DNA and microRNA sequences were dissolved in TE buffer (pH 8.0) according to manufacturer's recommendations. The buffer solutions employed in this study were listed in Supplementary materials.

Electrochemical impedance spectroscopy (EIS) was carried out with a CHI660C electrochemistry workstation (Austin, USA) in 5.0 mM $Fe(CN)_6^{3-/4-}$ (1:1) solution containing 0.1 M KCl at an open circuit potential over a frequency range from 0.1 Hz to 100 kHz. A three-electrode electrochemical cell was composed of a modified ITO electrode as the working electrode, a platinum wire as the auxiliary electrode, and a saturated calomel electrode (SCE) as the reference electrode. Scanning electron microscopic (SEM) images were recorded by a Hitachi S4800 scanning electron microscope (Hitachi Corporation, Japan). Powder X-ray diffraction (XRD) was performed on a Bruker D8 Advance X-ray diffractometer (Germany) with Cu $K\alpha$ radiation ($k = 0.1542$ nm).

Photoelectrochemical measurements were performed with a homemade photoelectrochemical system with an optical filter of 450 nm. The light intensity was about 20 m W/cm^2 measured by a radiometer (Photoelectric Instrument Factory of Beijing Normal University, Beijing, China). Photocurrent was recorded on a CHI832A electrochemical workstation (Austin, USA) with a three-electrode system. A modified ITO electrode with an area of 0.195 cm^2 was used as the working electrode, a Pt wire as the counter electrode and an SCE as the reference electrode. A 0.1 M PBS (pH 7.8) was used as the blank solution for photocurrent measurements, which was degassed by nitrogen for 30 min before photoelectrochemical experiments.

2.2. PEC biosensor fabrication

The ITO slices were used as the working electrode, which were cleaned by immersion in ethanol/NaOH mixed solution (v/v, 1:1) and acetone successively with sonication for 30 min, followed by washing copiously with double distilled deionized water and dried at 60 °C for 2 h.

4 mg of Bi_2S_3 powder was weighed accurately and dispersed ultrasonically in 1 mL of double distilled deionized water, and then 40 μL of the suspension was dropped onto a piece of ITO electrode. After drying in air, the Bi_2S_3/ITO was ringed with double distilled deionized water for three times. Then, 40 μL of AuNPs was further dropped on the electrode surface and dried under infrared lamp, followed by rinsing with double distilled deionized water for three times (The electrode was noted as AuNPs/Bi_2S_3/ITO). Subsequently, AuNPs/Bi_2S_3/ITO was incubated with 20 μL of probe immobilization buffer containing 0.5 μM probe DNA S1 for 12 h under humid conditions. After rinsed with 10 mM Tris–HCl (pH 7.4) for three times, 20 μL of probe immobilization buffer containing 5 μM MPA was dropped on electrode surface and incubated for 1 h. The obtained electrode was noted as probe/AuNPs/Bi_2S_3/ITO.

MicroRNA hybridization was performed by incubating probe/AuNPs/Bi_2S_3/ITO electrode with 20 μL of microRNA hybridization buffer containing various concentrations of microRNA-21 for 3 h at 37 °C (noted as miRNA-probe/AuNPs/Bi_2S_3/ITO). After that, the 3′-end of probe DNA S1 was further hybridized with 0.5 μM capture DNA S2 for 2 h, which was dissolved in 20 μL of DNA hybridization buffer (noted as c-DNA/miRNA-probe/AuNPs/Bi_2S_3/ITO). Afterwards, the electrode was incubated with 20 μL PBS (0.1 M, pH 7.4) containing 1 mg/mL streptavidin for 1 h under humid conditions (the electrode was noted as Avidin/c-DNA/miRNA-probe/AuNPs/Bi_2S_3/ITO). Following that, 20 μL of 0.1% PEG3350 was dropped on the electrode surface to block any nonspecific reaction sites. Finally, the electrode was incubated with 20 μL of Bio-AA-Apo solution for 75 min, followed by rinsing with 10 mM Tris–HCl (pH 7.4). The electrode was indicated as Apo/Avidin/c-DNA/miRNA-probe/AuNPs/Bi_2S_3/ITO.

2.3. PEC detection

For optimization of Bi_2S_3 concentration, wavelength and applied potential, Bi_2S_3/ITO was used as working electrode. The PEC detection was carried out in 0.1 M PBS (pH 7.4) containing 0.1 M AA, which was served as a sacrificial electron donor during the photocurrent measurement. For optimization of other detection conditions, Apo/Avidin/c-DNA/miRNA-probe/AuNPs/Bi_2S_3/ITO was used as working electrode and 0.1 M PBS (pH 7.8) containing 1 μg/mL trypsase was used as detection buffer. Light excitation of 450 nm was switched every 10 s. The applied potential was 0.0 V.

For detection of microRNA-21, the fabrication PEC biosensor was first immersed into 0.1 M PBS (pH 7.8) containing 1 μg/mL trypsase for 3 min to make apoferritin disassociation. As a result, AA was released into the PBS as sacrificial electron donor. Then, the photocurrent was measured under light excitation (450 nm). The applied potential was 0.0 V.

2.4. Total RNA extraction and characterization

DF-1 chicken fibroblast cell line were seeded in 75 cm^2 well at a density of approximately 1×10^6 cells per well. ALV-J China strain (NX0101) were inoculated onto DF-1 cells and incubated at 37 °C for 2 h. Then the cells were cultured with fresh medium contained 1% fetal bovine serum (FBS, Invitrogen, CA, USA). Observed daily, on the seventh day of the post-inoculation, cells were collected and RNA was extracted from infected DF-1 cells using RNA extraction kit (TaKaRa, Dalian, China) according to manufacturer's recommended protocol. Total RNA was also extracted from hepatic tissue of ALV-J infected birds. Total RNA extracted from un-infected DF-1 cells and normal tissues were used as control. RNA concentration was determined by UV–vis spectrophotometry. RNA integrity was checked by TBE agarose gel electrophoresis analyzing integrity and relation of the 28 S rRNA, 18 S rRNA, and 5 S rRNA bands.

3. Results and discussion

3.1. Characterization of Bi_2S_3

The morphology of the synthesized Bi_2S_3 powder was investigated by SEM and displayed in Fig. 1A. It showed that the Bi_2S_3 powder mostly consisted of nanorods with diameter of tens of nanometers and length of a few hundred nanometers. The synthesized Bi_2S_3 powder was further characterized by XRD and the corresponding peaks were shown in Fig. 1B. The position and intensity of all the peaks were in good agreement with the reported powder diffraction file (JCPDS File No. of 17-0320).

3.2. Characterization of PEC biosensor

The fabrication process of the PEC biosensor was characterized by EIS and photoelectrochemical measurements. In EIS measurements,

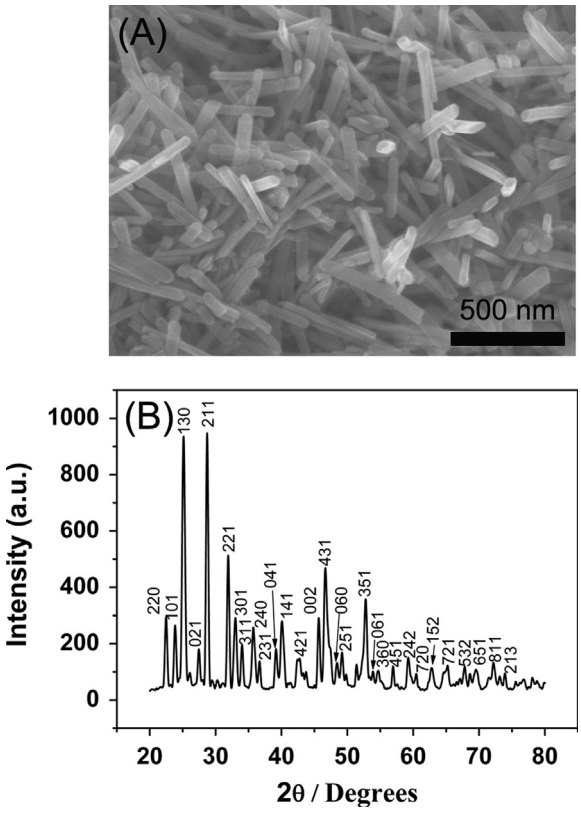

Fig. 1. The XRD pattern (A) and SEM image (B) of Bi_2S_3.

the electron-transfer resistance (R_{et}) which was equal to the semi-circle diameter reflected the restricted diffusion of the redox probe through the multilayer system related directly to the film permeability (Qian et al., 2010). Fig. S1 (see Supplementary materials) displayed the Nyquist diagrams of EIS in accordance with different electrode assembly processes. Obviously, Bi_2S_3/ITO (curve b) presented a small semi-circle in high-frequency region compared with the bare ITO electrode (curve a), indicating a low electron-transfer resistance. After AuNPs was electrodeposited on Bi_2S_3/ITO, the R_{et} decreased significantly (curve c). This decrease could be ascribed to the deposited AuNPs with high conductivity to promote the electron transfer rate from redox probe to electrode. In addition, AuNPs can further increase the effective electrode surface area and thus have the potential to anchor more DNA probes to amplify the signal (Yin et al., 2012b). However, the R_{et} increased when probe DNA S1 and MPA were assembled on AuNPs/Bi_2S_3/ITO surface (curve d), which could be explained as that the negatively charged phosphoric acid backbone of probe and carboxyl of MPA repelled the negatively charged $Fe(CN)_6^{3-/4-}$ and inhibit the electron transfer. The same phenomenon was also obtained after microRNA-21 (curve e) and capture DNA S2 (curve f) were hybridized with probe DNA S1 successively, which was also caused by the electrostatic repulsive-force between phosphate skeleton of oligonucleotide and redox probe. After the immobilization of streptavidin (curve g) and Bio-AA-Apo (curve h), the R_{et} increased in succession. This phenomenon was agreed with the fact that the protein layer was insulated and huge-volumed, which could block the interfacial electron transfer and increase the electron transfer resistance. This result testified the successful immobilization of AA loaded apoferritin on the electrode surface.

The fabrication of the PEC biosensor was also monitored by photoelectrochemical method in 0.1 M PBS (pH 7.8) containing 0.1 M AA. As shown in Fig. S2 (see Supplementary materials), there was no photocurrent detected on the bare ITO electrode (curve a). At Bi_2S_3/ITO (curve b), a strong photocurrent was obtained, which can be attributed to Bi_2S_3 nanorods compared with ITO electrode (no photocurrent was observed, curve a), indicating that Bi_2S_3 nanorods were excellent photoelectric conversion material. After immobilization of AuNPs onto Bi_2S_3/ITO, the photocurrent decreased (curve c). Then, the photocurrent further successively decreased with hairpin-structure probe immobilization (curve d), and hybridization with microRNA-21 (curve e) and capture DNA S2 (curve f). This phenomenon could be explained as two factors. One was the effect of steric hindrance resulting from immobilized oligonucleotides, which blocked AA to diffuse to the electrode surface. As a result, the photogenerated hole could not be effectively filled by the electron donated by AA, which made the photocurrent decreased. Another factor was the effect of electrostatic repulsion. As the pK_a of AA was 4.1 (Li et al., 2010), AA was controlled by negative charge in pH 7.4 PBS. The diffusion of AA towards electrode surface could be blocked by the negative charged DNA and microRNA. After the specific interaction between biotin at the 5′-end of capture DNA S2 and streptavidin, the photocurrent decreased (curve g), which might be ascribed to the large volume of streptavidin blocking the diffusion of AA. Finally, with immobilization of Bio-AA-Apo through the specific interaction between biotin in Bio-AA-Apo and the residual recognized sites in streptavidin, the photocurrent further decreased (curve h) with the same reason to the immobilization of streptavidin. These results also demonstrated that the successively fabrication of PEC biosensor. We also investigated the photoelectrochemical response of different electrodes in 0.1 M PBS (pH 7.8) without electron donor. As seen in Fig. 2A, the variation tendency of the photoelectrochemical response obtained at different electrodes was same to Fig. S2, which further demonstrated that the successively fabrication of PEC biosensor.

Fig. 2B showed the photoelectrochemical response of Apo/Avidin/c-DNA/miRNA-probe/AuNPs/Bi_2S_3/ITO in 0.1 M PBS (pH 7.8)

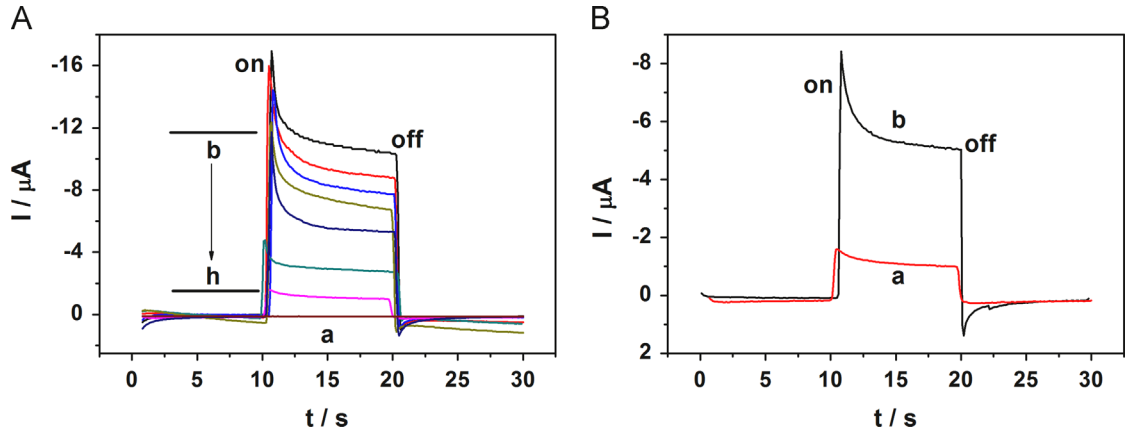

Fig. 2. (A) Photoelectrochemical response of different electrodes in 0.1 M PBS (pH 7.8). The applied potential was 0 V and the light wavelength was 450 nm. (a) ITO, (b) Bi_2S_3/ITO, (c) AuNPs/Bi_2S_3/ITO, (d) probe/AuNPs/Bi_2S_3/ITO, (e) miRNA-probe/AuNPs/Bi_2S_3/ITO, (f) c-DNA/miRNA-probe/AuNPs/Bi_2S_3/ITO, (g) Avidin/c-DNA/miRNA-probe/AuNPs/Bi_2S_3/ITO, (h) Apo/Avidin/c-DNA/miRNA-probe/AuNPs/Bi_2S_3/ITO. (B) Photoelectrochemical response of Apo/Avidin/c-DNA/miRNA-probe/AuNPs/Bi_2S_3/ITO in 0.1 M PBS (pH 7.4) in the absence (a) and presence (b) of 1 μg/mL trypsase.

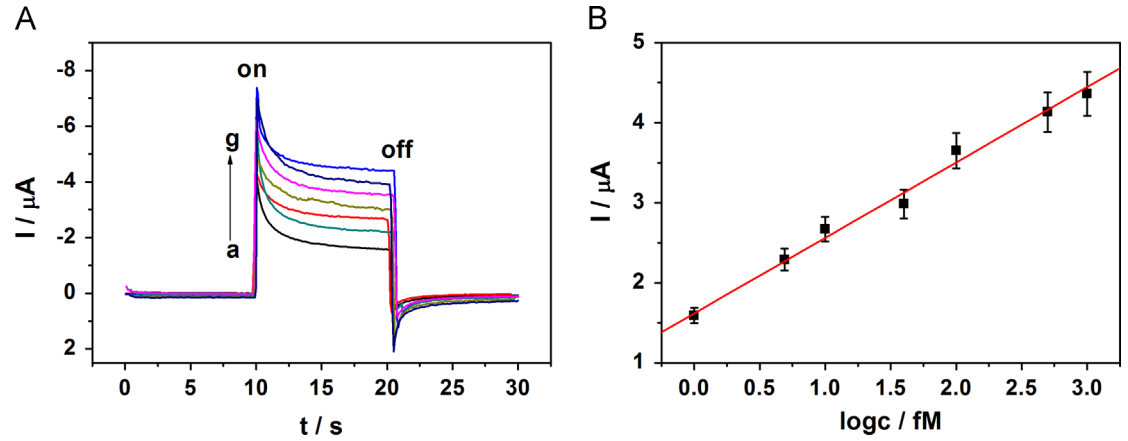

Fig. 3. (A) Photocurrent responses of the PEC biosensor hybridized with various concentrations of microRNA-21 in 0.1 M PBS (pH 7.8) containing 1 μg/mL trypsase. MicroRNA-21 concentration (a–g): 1, 5, 10 50, 100, 500, 1000 fM. (B) Calibration curve.

in the absence (curve a) and presence (curve b) of 1 μg/mL trypsase. The photoelectrochemical response increased significantly after the biosensor was treated with trypsase, indicating that the Bio-AA-Apo could be catalytically hydrolyzed by trypsase, and the loaded AA could be released from the cavity of apoferritin into the detection buffer as sacrifice electron donor to increase the current response. This result also demonstrated that the fabticated biosensor could be used to detect microRNA concentration using the increased photocurrent.

3.3. MicroRNA-21 detection performance

Under the optimal detection conditions (Figs. S3 and S4, see Supplementary materials), the calibration graph for the determination of microRNA-21 was shown in Fig. 3A and B. The change of the photocurrent was proportional to the logarithm of microRNA-21 concentrations in the ranges from 1–5000 fM with correlation coefficients of 0.9959. The regression equation was I (μA)=0.94log$c$ (fM) +1.62, and the detection limit was 0.35 fM (S/N=3). The detection limit of this method was lower than some of previous reports with different detection methods as listed in Table 1.

The selectivity of the fabricated PEC biosensor in discriminating completely complementary target microRNA-21 from single- and three-base mismatched, and non-complementary microRNA sequences was investigated under the concentration of 1 pM target microRNA. For achieving it, the differences between the photocurrent of Apo/Avidin/c-DNA/miRNA-probe/AuNPs/Bi_2S_3/ITO in 0.1 M PBS containing 1 μg/mL trypsase after light irradiation (where the probe was hybridized with complementary, single- and three-base mismatched, and non-complementary microRNA, respectively) and the photocurrent of probe/Bi_2S_3/ITO under same conditions were compared. As shown in Fig. S5 (see Supplementary materials), a strong photocurrent change was obtained for the complementary sequence. The signal change intensity of single- and three-base mismatched microRNA sequences was much weaker than that of the complementary microRNA sequences, and the non-complementary microRNA sequence showed even lower response change. The results showed that a good selectivity with this PEC biosensor for microRNA-21 detection was achieved.

The reproducibility of the PEC biosensor was evaluated by intra- and inter-assay coefficients of variation (CV). The microRNA-21 with concentration of 1 pM was repeatedly determined using the proposed biosensor for five times, intra-assay CV was 5.67%. The inter-assay CV on five biosensors was 5.42%. Considering order of magnitudes of the detection concentration of microRNA was pM, we think that the reproducibility of the PEC biosensor was satisfactory.

The stability of the photocurrent responses of the fabricated biosensor was also studied (Fig. S6, see Supplementary materials). No significant change of photocurrent response was observed with light on and off which was repeated 10 times over 200 s (RSD= 0.48%), indicating a good stability.

Table 1
The comparison of detection performance of the PEC biosensor with other detection methods.

Method	Linear range (M)	Detection limit (M)	Refs.
Electrochemistry	1.0×10^{-13}–1.0×10^{-8}	6.7×10^{-14}	(Dong et al., 2012a)
Electrochemistry	1.0×10^{-14}–2.0×10^{-12}	1.0×10^{-14}	(Wang et al., 2012a)
Electrochemistry	1.0×10^{-14}–7.0×10^{-10}	6.0×10^{-15}	(Yin et al., 2012a)
Electrochemistry	2.0×10^{-14}–1.0×10^{-11}	1.0×10^{-14}	(Gao and Peng, 2011)
Electrochemistry	1.0×10^{-13}–7.0×10^{-11}	6.0×10^{-14}	(Yin et al., 2012b)
Colorimetry	5.0×10^{-8}–1.0×10^{-16}	1.0×10^{-8}	(Zhang et al., 2009)
Piezoelectric cantilever biosensors	1.0×10^{-14}–1.0×10^{-19}	4.0×10^{-15}	(Johnson and Mutharasan, 2012)
Fluorescence	5.0×10^{-15}–5.0×10^{-12}	2.1×10^{-15}	(Dong et al., 2012b)
PEC biosensor	1.0×10^{-15}–5.0×10^{-12}	3.5×10^{-16}	This work

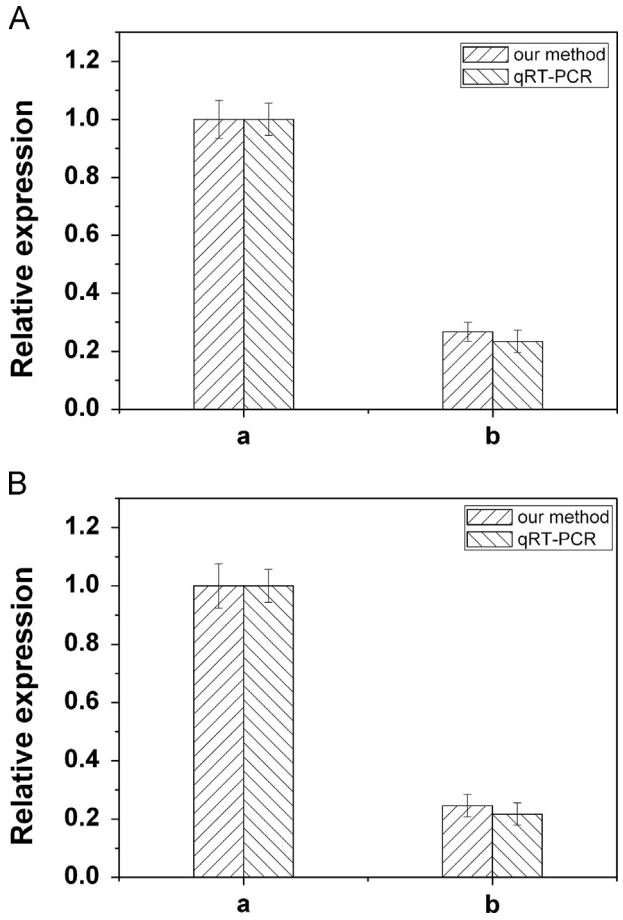

Fig. 4. The relative expression level of microRNA-21 in liver tissue of chicken (A) and DF-1 chicken fibroblast cell (B) obtained by photoelectrochemical method and qRT-PCR. Column a is normal tissue and cell. Column b is tissue and cell infected with ALVs.

3.4. MicroRNA-21 expression in real samples

With the high sensitivity and selectivity, the immunosensor allowed us to directly and PCR-freely analyze microRNA expression in total RNA extracted from cells and tissues. For confirming it, the expression level change of microRNA-21 in chicken cells and liver tissues infecting with ALVs was investigated. For achieving it, the total RNA was first extracted from cells and issues with and without infecting ALVs. The integrity of the total RNA was confirmed by agarose gel electrophoresis. The three bands of 28 S, 18 S and 5 S were obtained, indicating the integrity of total RNA. The ratio of A_{260} and A_{280} was 1.878, 1.769, 1.902 and 1.821 for normal and diseased cells and tissues, respectively, implying the relative high purity of total RNA. As seen in Fig. 4, the expression level of microRNA-21 was decreased in diseased cells and tissues compared normal cells and tissues, which was in accordance with the detection results obtained from qRT-PCR. This result indicated that microRNA-21 might serve as a new biomarker in avian leukosis diagnosis.

4. Conclusions

Herein, we have demonstrated a sensitive and selective photoelectrochemical biosensing protocol for monitoring the expression level change of microRNA in cells and tissues infecting with ALVs based on the use of nanometersized Bi_2S_3 coupled with ITO. Taking the advantages of apoferritin that the protein cage can be disassociated when pH is lower than 2.0 and recombined when pH is higher than 8.5, AA was loaded into the cavities of apoferritin. The AA loaded apoferritin immobilized on ITO surface could release AA into the detection buffer as electron donor in the presence of trypsase, which would lead to an increased photocurrent. The developed assay method showed high detection sensitivity and specificity. The sample detection results indicated that microRNA might be regarded as a new biomarker in avian leukosis.

Acknowledgments

This work was supported by the National Natural Science Foundation of China (Nos. 21075078, 21105056) and the Natural Science Foundation of Shandong province, China (Nos. ZR2010BM005, ZR2011BQ001).

Appendix A. Supplementary material

Supplementary data associated with this article can be found in the online version at http://dx.doi.org/10.1016/j.bios.2013.09.053.

References

Bessekhouad, Y., Robert, D., Weber, J.V., 2004. Journal of Photochemistry and Photobiology A: Chemistry 163 (3), 569–580.
Cissell, K.A., Rahimi, Y., Shrestha, S., Hunt, E.A., Deo, S.K., 2008. Analytical Chemistry 80 (7), 2319–2325.
Ding, C., Li, H., Li, X., Zhang, S., 2010. Chemical Communications 46 (42), 7990–7992.
Dong, D., Dong, Z., Wang, F.-Q., Yang, X.-Q., Wang, N., Li, Y.-G., Guo, L.-H., Cheng, J., 2004. Analytical Chemistry 76 (2), 499–501.
Dong, H., Jin, S., Ju, H., Hao, K., Xu, L.-P., Lu, H., Zhang, X., 2012a. Analytical Chemistry 84 (20), 8670–8674.
Dong, H., Zhang, J., Ju, H., Lu, H., Wang, S., Jin, S., Hao, K., Du, H., Zhang, X., 2012b. Analytical Chemistry 84 (10), 4587–4593.
Gao, Z., Peng, Y., 2011. Biosensors and Bioelectronics 26 (9), 3768–3773.
Ge, Z.-H., Zhang, B.-P., Yu, Z.-X., Jiang, B.-B., 2012. CrystEngComm 14 (6), 2283–2288.
Gong, J., Wang, X., Li, X., Wang, K., 2012. Biosensors and Bioelectronics 38 (1), 43–49.

Harrison, P.M., Arosio, P., 1996. Biochimica et Biophysica Acta (BBA) – Bioenergetics 1275 (3), 161–203.
Hatai, H., Ochiai, K., Umemura, T., 2009. Journal of Veterinary Diagnostic Investigation 21 (4), 519–522.
Huang, G.L., Zhang, X.H., Guo, G.L., Huang, K.T., Yang, K.Y., 2009. Oncology Reports 21 3, 673–679.
Johnson, B.N., Mutharasan, R., 2012. Analytical Chemistry 84 (23), 10426–10436.
Kang, Q., Yang, L., Chen, Y., Luo, S., Wen, L., Cai, Q., Yao, S., 2010. Analytical Chemistry 82 (23), 9749–9754.
Li, F., Chai, J., Yang, H., Han, D., Niu, L., 2010. Talanta 81 (3), 1063–1068.
Li, H., Li, J., Yang, Z., Xu, Q., Hu, X., 2011. Analytical Chemistry 83 (13), 5290–5295.
Liao, N., Zhuo, Y., Chai, Y., Xiang, Y., Cao, Y., Yuan, R., Han, J., 2012. Chemical Communications 48 (61), 7610–7612.
Liu, G., Wang, J., Wu, H., Lin, Y., 2006a. Analytical Chemistry 78 (21), 7417–7423.
Liu, G., Wu, H., Wang, J., Lin, Y., 2006b. Small 2 (10), 1139–1143.
Liu, J., Lu, Y., 2006. Nature Protocols 1 (1), 246–252.
Lu, W., Jin, Y., Wang, G., Chen, D., Li, J., 2008. Biosensors and Bioelectronics 23 (10), 1534–1539.
Lu, W., Wang, G., Jin, Y., Yao, X., Hu, J., Li, J., 2006. Applied Physics Letters 89 (26), 263902.
Medina, P.P., Slack, F.J., 2008. Cell Cycle 7 (16), 2485–2492.
Mohammadi, A., Asasi, K., Masoudian, M., Bozorgchami, B., 2008. Iranian Journal of Veterinary Research 9 (3), 24.
Pöhlmann, C., Sprinzl, M., 2010. Analytical Chemistry 82 (11), 4434–4440.
Peter, L.M., Wijayantha, K.G.U., Riley, D.J., Waggett, J.P., 2003. The Journal of Physical Chemistry B 107 (33), 8378–8381.
Qian, Z., Bai, H.-J., Wang, G.-L., Xu, J.-J., Chen, H.-Y., 2010. Biosensors and Bioelectronics 25 (9), 2045–2050.
Robert, D., 2007. Catalysis Today 122 (1-2), 20–26.
Sun, B., Zhang, K., Chen, L., Guo, L., Ai, S., 2013. Biosensors and Bioelectronics 44 (0), 48–51.
Tahir, A.A., Ehsan, M.A., Mazhar, M., Wijayantha, K.G.U., Zeller, M., Hunter, A.D., 2010. Chemistry of Materials 22 (17), 5084–5092.
Tu, W., Dong, Y., Lei, J., Ju, H., 2010. Analytical Chemistry 82 (20), 8711–8716.
Wang, G.-L., Xu, J.-J., Chen, H.-Y., 2009. Biosensors and Bioelectronics 24 (8), 2494–2498.
Wang, J., Yi, X., Tang, H., Han, H., Wu, M., Zhou, F., 2012a. Analytical Chemistry 84 (15), 6400–6406.
Wang, P., Ma, X., Su, M., Hao, Q., Lei, J., Ju, H., 2012b. Chemical Communications 48 (82), 10216–10218.
Webb, B., Frame, J., Zhao, Z., Lee, M.L., Watt, G.D., 1994. Archives of Biochemistry and Biophysics 309 (1), 178–183.
Wu, X., Chai, Y., Yuan, R., Su, H., Han, J., 2013. Analyst 138 (4), 1060–1066.
Yan, L.-X., Huang, X.-F., Shao, Q., Huang, M.-Y., Deng, L., Wu, Q.-L., Zeng, Y.-X., Shao, J.-Y., 2008. RNA 14 (11), 2348–2360.
Yang, H., Hui, A., Pampalakis, G., Soleymani, L., Liu, F.-F., Sargent, E.H., Kelley, S.O., 2009. Angewandte Chemie International Edition 48 (45), 8461–8464.
Yang, L., Liu, C., Ren, W., Li, Z., 2012. ACS Applied Materials and Interfaces 4 (12), 6450–6453.
Yin, H., Zhou, Y., Chen, C., Zhu, L., Ai, S., 2012a. Analyst 137 (6), 1389–1395.
Yin, H., Zhou, Y., Zhang, H., Meng, X., Ai, S., 2012b. Biosensors and Bioelectronics 33 (1), 247–253.
Zhang, X., Li, S., Jin, X., Zhang, S., 2011. Chemical Communications 47 (17), 4929–4931.
Zhang, X., Liao, M., Jiao, P., Luo, K., Zhang, H., Ren, T., Zhang, G., Xu, C., Xin, C., Cao, W., 2010. Journal of Clinical Microbiology 48 (6), 2116–2121.
Zhang, X., Xu, Y., Zhao, Y., Song, W., 2012a. Biosensors and Bioelectronics 39 (1), 338–341.
Zhang, Y., Li, Z., Cheng, Y., Lv, X., 2009. Chemical Communications 22, 3172–3174.
Zhang, Y., Zhang, C.-y., 2012. Analytical Chemistry 84 (1), 224–231.
Zhang, Z., Wang, W., Wang, L., Sun, S., 2012b. ACS Applied Materials and Interfaces 4 (2), 593–597.